Chemical Engineering Science 195 (2019) 120–126

Contents lists available at ScienceDirect

Chemical Engineering Science

journal homepage: www.elsevier.com/locate/ces

A new non-dimensional parameter to obtain the minimum mixing length in tree-like concentration gradient generators

Milad Rismanian [a], Mohammad Said Saidi [a,1], Navid Kashaninejad [b,1]

[a] Department of Mechanical Engineering, Sharif University of Technology, 11155-9567 Tehran, Iran
[b] School of Mathematical and Physical Sciences, University of Technology Sydney, Sydney, New South Wales 2007, Australia

HIGHLIGHTS

- A novel parameter was defined for designing a concentration gradient generator (CGG).
- The parameter is constant and independent of the flow rate and channel dimensions.
- It greatly facilitates efficient designing of a CGG.

ARTICLE INFO

Article history:
Received 18 July 2018
Received in revised form 16 November 2018
Accepted 18 November 2018
Available online 19 November 2018

Keywords:
Concentration gradient generator
Mixing length
Peclet number
Micromixer

ABSTRACT

Microfluidic-based concentration gradient generators (CGGs) have a number of applications in chemical, biological and pharmaceutical studies. Thus, precise design of the microfluidic system is crucial to maintaining the desired concentration gradient in microchannels. One of the design considerations is the length of microchannels in the structure of a CGG. A CGG with a short length fails to provide the complete diffusive mixing, while the size of the microchip would unfavorably increase by incorporating a long CGG. Considering a CGG as a tree-like structure consisting of T-shaped micromixers, the mixing process of the species at a straight microchannel has been solved analytically. Herein, we define a new non-dimensional parameter (ψ) as the ratio of the minimum length of the microchannel required for the desired fluid mixing to the product of the channel width and Peclet number. The numerically obtained values of ψ (i.e., 0.22 and 0.17 for 95% mixing in straight and serpentine micromixers, respectively) are in good agreement with the experimental results. The numerical simulation also shows that the value of ψ is the same for all micromixers in a CGG with the similar microchannel structure (e.g., straight or serpentine) and is independent of the channel size (width-to-depth ratio) and fluid velocity. Therefore, ψ can be computed only once for any micromixer with different structures (e.g., zigzag, square wave, and so forth) and then considering this constant value of ψ, the minimum required length of all other micromixers in a CGG with similar repetitive structures and dimensions at the specified flow rates could be designed quickly and precisely.

1. Introduction

Over the past decade, microfluidic technology has shown great promise to revolutionize the current practice in chemistry (Chiu et al., 2017), biology (Duncombe et al., 2015; Linshiz et al., 2016; Zilionis et al., 2017), biomedicine (Khademhosseini and Langer, 2016; Sackmann et al., 2014) and other branches of science (Kashaninejad et al., 2016; 2018; Liu, 2011; Nimafar et al., 2012; Wang et al., 2012; 2017). One of the most common applications of microfluidics is examining the effect of different reagents and their concentrations in a microenvironment for monitoring the cellular reaction and drug screening (Moghadas et al., 2017; Nguyen et al., 2013). To this aim, concentration gradient generators (CGGs) should be integrated in such microfluidic devices to precisely generated the desired range of the concentrations of the reagents (Jeon et al., 2002; Wang et al., 2004).

One of the most popular CGG designs consists of a series of micromixers, where the required concentrations are generated. There are two approaches to the design and fabrication of a CGG: partial mixing and complete mixing of the fluids in the micromixers. In CGGs with partial mixing, mass transport, momentum, and continuum equations are simultaneously solved at each micromixer

[1] These authors contributed equally to this work.

https://doi.org/10.1016/j.ces.2018.11.041
0009-2509/

to obtain the outlet concentration (Wang et al., 2006). Although this approach is useful to estimate the concentration gradient of the fluid at the outlet of a CGG, it cannot be used to design a CGG to generate a particular concentration gradient directly. In the complete mixing approach, the flow rate and the average fluid concentration in each micromixer are calculated using hydrodynamics equations and electrical analogy (Toh et al., 2014). The central assumption in this approach is the complete mixing of the fluids at the outlet of each micromixer. As such, the length of the mixing channel must be long enough. Since the required length is a function of flow rate and dimensions of the mixing channel, finding a straightforward method to estimate the required mixing length is very crucial.

In this regard, Jeon and colleagues proposed that linear concentration gradients can be generated with a symmetric microchannel network with two inlets (Jeon et al., 2000). Dertinger et al. extended their design by creating the gradients with complex shapes (including linear, parabolic and periodic) using networks of microchannels, which were spatially and temporally stable (Dertinger et al., 2001). Similarly, a three-inlet CGG to generate a polynomial gradient was proposed (Chung et al., 2005). Later, Lin and colleagues presented an extended microdevice by adding two mixer inlets to the gradient generating network (Lin et al., 2004). In that design, the flow rates could be independently controlled by syringe pumps to generate temporal and spatial concentration gradients. Walker and others (Walker et al., 2005) used simplified numerical model and experiments to investigate the stability of the linear concentration gradient generated by a CGG composed of two inlets and four outlets.

In order to generate an intended concentration gradient in a direction perpendicular to the direction of the fluid flow, a tree-like structure is commonly used. In a tree-like CGG, two solutions with different concentrations meet each other at a T-junction and are combined. These junctions are repeated, and finally, the desired concentration gradient across the main microchannel is generated based on the controlled diffusive mixing of laminar flow (Lee et al., 2011). Samples with different concentrations should be completely mixed to generate a uniform concentration along the width of the channel before splitting so that the electrical analogy can be used. Because of low Peclet number ($Pe = UL/D$, where U, L, and D are respectively the average fluid velocity, the width of the microchannel, and the diffusion coefficient) in microchannels, the diffusion process is the dominant mechanism of mixing, which is an inherently slow process. As such, rapid mixing in microchannels is necessary to reduce the characteristic length of the microfluidic device. This is challenging for the systems with high flow rates or low diffusion coefficients. To overcome this limitation, passive and active mixers have been developed (Suh and Kang, 2010). Passive mixing can be obtained by increasing the contact area between the mixing species by changing the microchannel configurations such as serpentine or zigzag structures while active mixers enhance the mixing by external forces such as magnetic or electric field (Lee et al., 2011). One of the initial steps in designing passive CGGs is the estimation of the channel length required to thoroughly mix the fluid in each branch of the device. This step is often performed by employing numerical solutions, which are difficult and time-consuming especially when the number of micromixers increases.

Fig. 1 shows a T-junction where one inlet stream with unity concentration ($c = 1$) enters the main channel and mixes with another inlet stream with zero concentration ($c = 0$). L and w are the width and depth of the channel respectively, and h is the initial width of the stream with unity concentration. Depending on the flow rate of the inlet streams, sample concentrations in the width of $0 \leqslant y < h$ and $h \leqslant y < L$of the inlet of the main channel are assumed to be one and zero, respectively. $h/L = 0.5$ corresponds to the case where the flow rates of both streams are equal. There are several mathematical solutions for specifying the concentration distribution in similar mixing systems (Jeon et al., 2000; Wu and Nguyen, 2005; Wu et al., 2004). Eq. (1) is the result of the first analytical solution that expresses the spatial concentration distribution of the main channel (Jeon et al., 2000):

$$c(x,y) = \frac{1}{2}\sum_{n=-\infty}^{\infty}\left[erf\left(\frac{h/L+2n-y/L}{2\sqrt{Dx/L^2\bar{u}}}\right)+erf\left(\frac{h/L-2n+y/L}{2\sqrt{Dx/L^2\bar{u}}}\right)\right] \quad (1)$$

where erf stands for error function and L, D and $\bar{u}$ represent the microchannel width, diffusivity and average fluid velocity in the mixing microchannel, respectively. The percent of mixing along the channel is defined by Eq. (2) (Jeon et al., 2000).

$$mixing(x) = 1 - \frac{\int_{y=0}^{L}|c(x,y)-c(\infty,y)|dy}{\int_{y=0}^{L}|c(0,y)-c(\infty,y)|dy} \quad (2)$$

Since in Eq. (1) the concentration is not expressed explicitly, the integrals in Eq. (2) should be evaluated numerically. Knowing the concentration at infinity ($c(x=\infty) = h/L$) and considering I terms in the sum, one can find the percentage of mixing as follows:

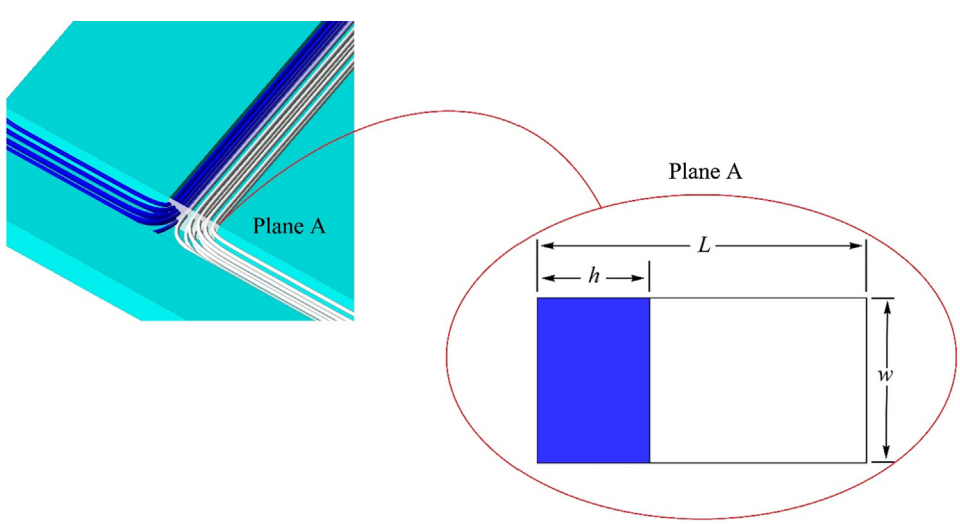

Fig. 1. Schematic representation of mixing two different concentration streams; Plane A is a cross-sectional view of the entrance of the mixing microchannel, w and L are depth and width of the channel, respectively. The initial width of the stream with unity concentration is shown by h.

$$mixing(x) = 1 - \frac{\sum_{i=1}^{I} \left|c(x, y_i) - \frac{h}{L}\right| \frac{L}{I}}{2h(1 - \frac{h}{L})} \tag{3}$$

The micromixers in different generations of a CGG usually have the same microchannel structure (straight, curved, and so on), and the same fluid flows in all the microchannels while flow rate and channel dimensions may vary. As such, the numerical procedure to find the minimum length required to achieve the desired mixing length for all of the micromixers is computationally expensive. In this study, we introduce a new non-dimensional parameter for the quick estimation of the concentration distribution and mixing length in a straight channel. The non-dimensional values are numerically calculated for the straight and serpentine micromixers and validated by the experimental data. By considering the same structure and fluid in the microchannels, the numerical simulation shows that this non-dimensional parameter is constant for all the micromixers in a typical CGG. The results also confirm that this parameter is independent of the flow rate or the channel sizes (the ratio of channel width to depth).

2. Methodology

To find the length required for the desired mixing in a T-shaped micromixer, analytical equations for convective-diffusive mass transport are solved using the method of separation of variables.

2.1. Analytical solution

Assuming a steady-state and parallel flow, the 3D governing equation for mass transport in the microchannel shown in Fig. 1 can be expressed by Eq. (4):

$$u\frac{\partial c}{\partial x} = D\left(\frac{\partial^2 c}{\partial x^2} + \frac{\partial^2 c}{\partial y^2} + \frac{\partial^2 c}{\partial z^2}\right) \tag{4}$$

where c stands for the mass concentration. By neglecting the entry region of the microchannel, the fluid flow can be assumed fully developed within the channel. We also assume that the velocity (u) in Eq. (4) can be replaced by the average velocity of the channel ($u \to U$). Moreover, by assuming small Peclet number, the diffusion along the channel length can be neglected compared to that across the channel width or depth by using the order-of-magnitude analysis. Finally, the boundary conditions of this problem can be specified as follows:

$$\begin{aligned} c|_{x=0} &= \begin{cases} 1 & 0 \leqslant y < h \\ 0 & h \leqslant y \leqslant L \end{cases} \\ \left.\frac{\partial c}{\partial y}\right|_{y=0} &= \left.\frac{\partial c}{\partial y}\right|_{y=L} = 0 \\ \left.\frac{\partial c}{\partial z}\right|_{z=0} &= \left.\frac{\partial c}{\partial z}\right|_{z=w} = 0 \end{aligned} \tag{5}$$

By applying the separation of variables method with the even expansion of the inlet boundary condition, the concentration distribution in the solution domain can be obtained, Eq. (6).

$$c(x, y) = \frac{h}{L} + \sum_{n=1}^{\infty} \frac{2}{n\pi} \sin\left(n\pi\frac{h}{L}\right) cos\left(n\pi\frac{y}{L}\right) exp\left[-n^2\pi^2\frac{Dx}{L^2U}\right] \tag{6}$$

Considering Eq. (6), one can observe that the ratio of the second term to the first term of the series is about 5×10^{-2}, and this ratio for the subsequent terms becomes considerably smaller. Therefore, the concentration distribution can be approximated as Eq. (7):

$$c(x, y) \approx \frac{h}{L} + \frac{2}{\pi} \sin\left(\pi\frac{h}{L}\right) cos\left(\pi\frac{y}{L}\right) exp\left[-\pi^2\frac{Dx}{L^2U}\right] \tag{7}$$

Combining, Eqs. (7) and (2), one can find the mixing fraction as Eq. (8):

$$mixing(x) = 1 - \frac{2}{\pi^2} \frac{\sin(\pi\frac{h}{L}) exp\left[-\pi^2\frac{Dx}{L^2U}\right]}{\frac{h}{L}(1 - \frac{h}{L})} \tag{8}$$

According to Eq. (8), the dimensionless number required to achieve 95% mixing (ψ) in a straight microchannel can be found from Eq. (9):

$$\psi = -\frac{1}{\pi^2} Ln\left[\frac{\pi^2}{40}\frac{h}{L}\left(1 - \frac{h}{L}\right) csc^{-1}\left(\pi\frac{h}{L}\right)\right] \tag{9}$$

where ψ is defined as:

$$\psi = \frac{x_{mixing}D}{L^2U} = \frac{x_{mixing}Dw}{LQ} = \frac{1}{Pe}\frac{x_{mixing}}{L} \tag{10}$$

In the above equation, $Q = ULw$, $Pe = LU/D$ are respectively the volumetric flow rate and Peclet number, and x_{mixing} represents the corresponding mixing length.

2.2. Numerical simulation

To validate the analytical solution and investigate the effect of flow profile on mixing length, numerical simulations based on the finite volume method are used. These numerical simulations are performed in two types of straight and serpentine T-shaped micromixers.

The schematic of the straight T-shaped micromixer used in the simulation is shown in Fig. 2a. The microchannel depth has been assumed to be 0.3 mm. A structured grid mesh has been generated for all the simulations, and its size has been selected after performing the grid independence analysis (Fig. 2b).

Fig. 2c shows the geometry of the serpentine T-shaped micromixer used in the simulation. The microchannel depth has been assumed to be 0.3 mm. In this micromixer, the mixing length is measured with a straight line from the microchannel inlet to the microchannel outlet, while the effective mixing length is measured along the flow path. The structured mesh constructed for this model is shown in Fig. 2d.

Since the Reynolds number in these microchannels is small, the simulations were carried out in a laminar condition. The second-order scheme was used to discretize the momentum and scalar transport equations. For the inlet boundary condition, the inlet velocity and constant concentration were applied. It was assumed that water flowed from each of the inlet vertical microchannels with a flow rate of 3 μl/min. So, the flow rate in the main horizontal microchannel was 6 μl/min. The fluid in the upper microchannel was assumed to have a concentration of unity while the concentration of the fluid from the lower microchannel was assumed to be zero (pure water). Constant pressure was applied at the outlet of the main microchannel. The physical properties of pure water were considered for the simulations, viz., fluid density and dynamic viscosity were assumed to be 1000 kg/m^3 and 0.001 kg/(m s), respectively, and the diffusion coefficient of the dye was estimated as 2.34e−9 m^2/s (Wan, 1965).

2.3. Experimental method

The micromixers were fabricated using standard soft lithography technique. In brief, a poly(methyl methacrylate) (PMMA) master mold was first fabricated using the micro machining technique with an accuracy of 10 μm. Then, polydimethylsiloxane (PDMS) was prepared by mixing the pre-polymer and its curing agent with the ratio of 10–1 and casted on the PMMA master mold to fabricate the top and bottom layers of the microfluidic system, comprising both straight and serpentine micromixers. Then, the PDMS molds were placed in an oven at 90 °C for 90 min. Finally, two layers were

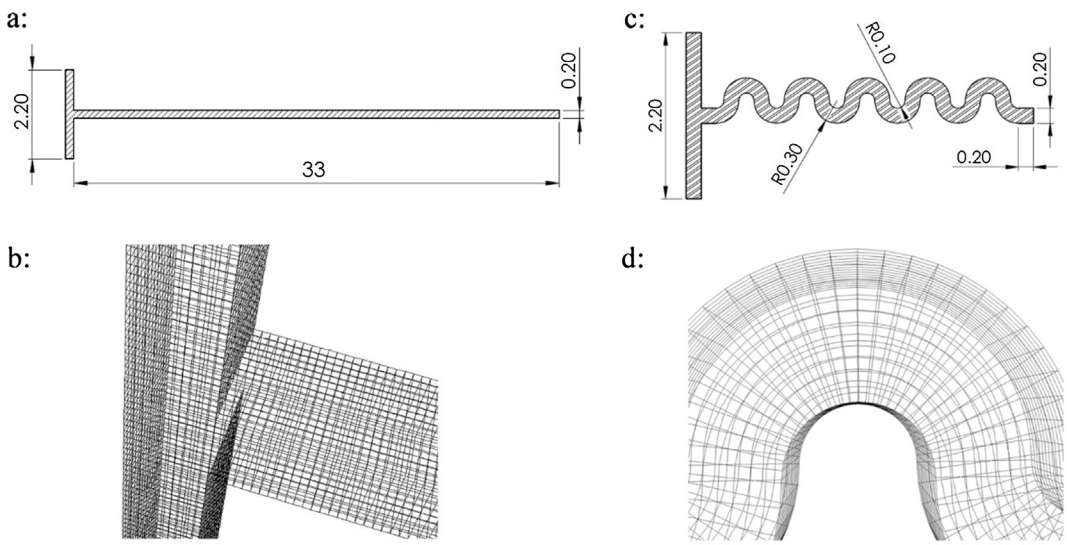

Fig. 2. a: Schematic of the straight T-shaped micromixer used for the numerical simulation; The units are in mm; b: The structured mesh generated for the straight T-shaped micromixer; c: Schematic of the serpentine T-shaped micromixer used for the numerical simulation; d: The structured mesh constructed for the serpentine T-shaped micromixer. All the units are in mm.

bonded via oxygen plasma treatment. The fabricated microfluidic system is shown in Fig. 3a.

To inject the fluid into the microfluidic system with a certain velocity, a syringe pump was used. Deionized water with a flow rate of 3 μl/min from one inlet and a diluted solution of Rhodamine B with a concentration of 10^{-6} g/g (water) with a flow rate of 3 μl/min from another inlet was injected. Then, the mixing of the two fluids was visualized by fluorescent images using an inverted fluorescent microscope. The concentration distribution of the fluids was measured using the standard image processing technique. The schematics of this setup is shown in Fig. 3b.

3. Results and discussion

3.1. Maximum mixing length

It can be deduced from Eq. (10) that the dimensionless mixing length (the dimensionless length required to achieve 95% mixing) is a function of h/L. This parameter represents the ratio of the upper to lower flow rates of the microchannels. Knowing the ratio of the flow rate between two combining streams (h/L), one can find the dimensionless mixing length from Eq. (9). In Fig. 4, the dimensionless mixing length is plotted against h/L. As shown, if h/L is 0.5, i.e., the flow rates of two inlet streams are equal, the dimensionless mixing length would be maximized at $\psi = 0.28$. Hence, from Eq. (10), the maximum mixing length in micromixer could be obtained as follows:

$$x_{95\%mixing} = 0.28\frac{QL}{wD} \tag{11}$$

where Q and w stand for volumetric fluid flow rate and microchannel depth, respectively.

Although h/L is not necessarily equal to 0.5 in the T-junctions of a microstructure, the maximum length required for 95% mixing in straight microchannels could be evaluated by this explicit equation.

3.2. Numerical results for a straight T-shaped micromixer

To investigate the effect of the 3D structure of the flow on the dimensionless mixing length, the computational fluid dynamic (CFD) simulation is performed on the straight T-shaped micromixer shown in Fig. 2a. The concentration distribution in T-shaped micromixer is shown in Fig. 5a.

Fig. 5b compares the results of the percentage of mixing obtained from the CFD simulation with those obtained from the analytically derived equation (Eq. (8)). These results show that the dimensionless mixing length (required to 95% mixing) obtained analytically is 27% larger than the numerically obtained one. This difference between the numerical and the analytical results can be the result of neglecting the entry region and substituting the average velocity in our proposed analytical solution. As such, the analytical approach slightly overestimates the mixing length. So, using the analytical relation proposed in this study, the minimum mixing length of the micromixer can be approximated with a safety margin.

3.3. Serpentine T-shaped micromixer

One of the common methods to decrease the mixing length (and consequently the overall size of the microfluidic device) is bending the path of fluid flow. To study the effect of this effect on the improvement of the mixing, fluid flow and mass transport in the serpentine T-shaped micromixer, shown in Fig. 2c, were simulated using CFD method. As shown, the straight length of this microfluidic system is 4.40 mm, while the total stream path length is 6.68 mm. Thus, with the benefit of serpentine micromixer, the length of this microfluidic device was reduced by 34.1%.

The results of this simulation for dimensionless concentration is shown in Fig. 6a. As shown in Fig. 6b, the mixing occurs more rapidly in the serpentine micromixer than those in the straight micromixer.

In Fig. 6b, the effective mixing length obtained from CFD simulation of serpentine T-shaped micromixer is compared with the straight one. The effective mixing length in the serpentine micromixer is 0.17, while it is 0.22 in the straight micromixer. As such, the effective mixing length was reduced approximately 23% by using a serpentine micromixer.

3.4. Experimental validation

Fig. 7 compares the CFD and the experimental results for the mixing fraction along the microchannel for the straight and ser-

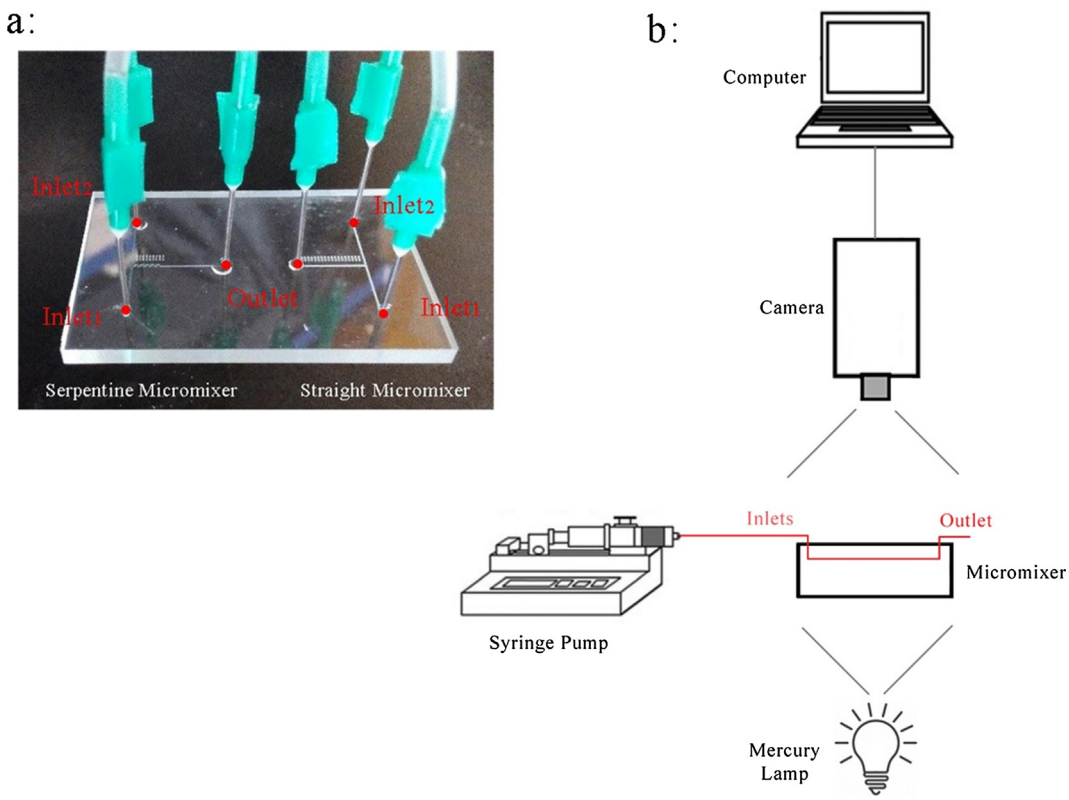

Fig. 3. Serpentine and straight micromixers in a microfluidic system; a: The image of the PDMS fabricated straight and serpentine micromixers, each of them has two fluid inlets and one outlet; b: The schematics of the experimental setup. The fluid flows through the micromixer using a syringe pump, and the concentration of the dye (Rhodamine B) was measured from a fluorescent microscope using image processing technique.

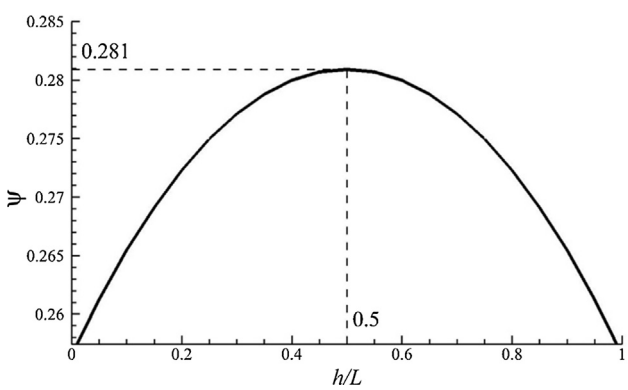

Fig. 4. Variation of the dimensionless mixing length with h/L. The maximum pressure corresponds to $\psi = 0.281$ and occurs when the flow rates of two inlet streams are equal ($h/L = 0.5$).

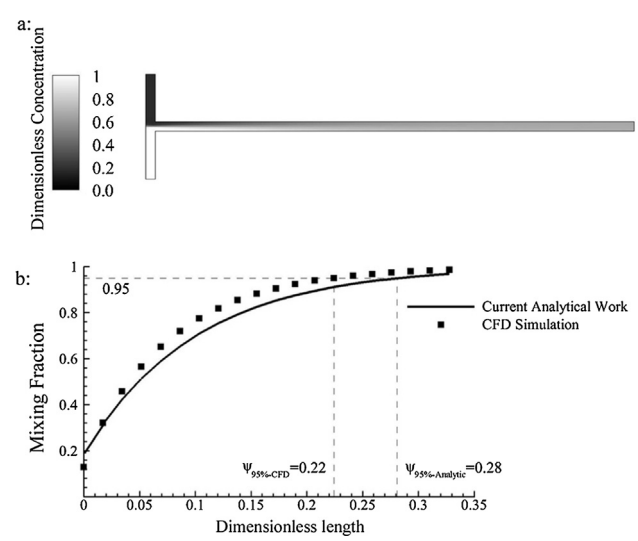

Fig. 5. a: Dimensionless concentration contours in the straight T-shaped micromixer obtained from numerical simulation; b: Comparison of numerical and analytical results of the mixing fraction along the length of the straight T-shaped micromixer as a function of the proposed non-dimensional mixing parameter.

pentine T-shape micromixers. As shown, there is a excellent agreement between the numerical and experimental results for both cases. The root-mean-square relative errors are 3.5% and 5.1% for straight and serpentine micromixers, respectively.

3.5. Effect of different parameters on ψ

As mentioned, a CGG (2D or 3D) commonly consists of a series of micromixers with geometrical similarity, Fig. 8. To ensure the complete mixing of two fluid streams entering each micromixer, the required mixing length of each micromixer should be computed. In each branch of a CGG, the flow rate and the structure (and even the cross-sectional area) of each micromixer may be different. Since the resultant CGGs may have a large number of micromixers with more geometrical complications, numerical simulation to find the mixing length for each micromixer with different flow rate or dimension is computationally expensive.

It should be investigated whether ψ depends on the geometric or hydrodynamic parameters of each individual micromixer. For this purpose, a typical micromixer, shown in Fig. 2a, was simulated using the conditions described in Section 2.2. The depth and the main channel flow rate of the micromixer were assumed to be

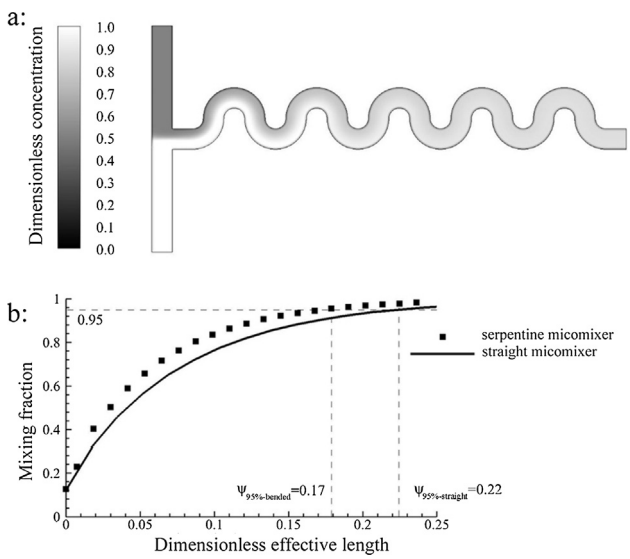

Fig. 6. a: Dimensionless concentration contours in the straight T-shaped micromixer; b: Mixing fraction along the length of the straight and serpentine T-shaped micromixer obtained from CFD simulation.

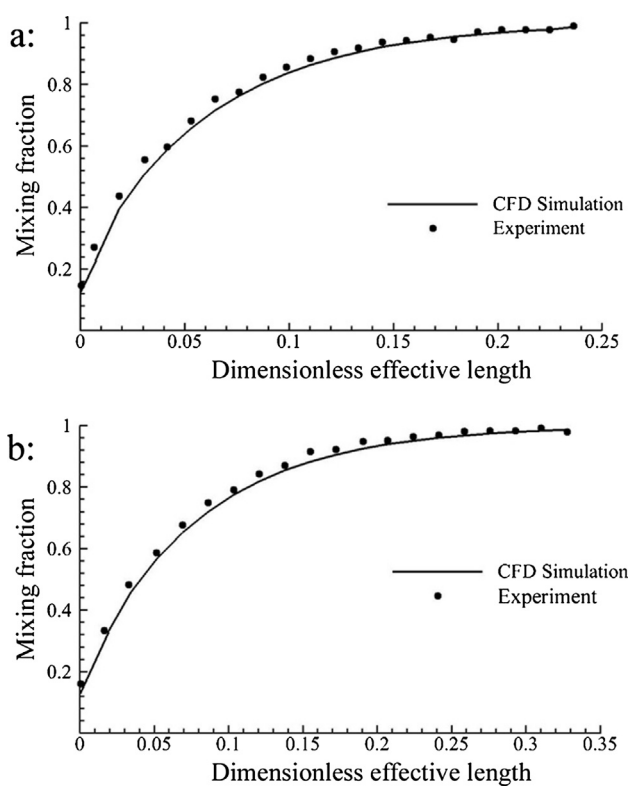

Fig. 7. Comparison of the mixing fraction along the length of the T-shaped micromixer obtained from the CFD simulation and the experiment for a: serpentine and b: straight micromixer.

0.3 mm and 6 μl/min, respectively. The dimensionless mixing length ψ, required to 95% mixing, was calculated 0.22 as expected according to Fig. 5b. Subsequently, we performed a set of 24 simulations in which the depth of the channel was varied from 0.06 to 1.5 mm. Assuming constant ψ, the corresponding mixing length in each channel was calculated by Eq. (10). It was investigated whether the mixing fraction in the calculated mixing length of the channel (constant ψ) differs from 0.95. The ratio of calculated mixing fraction to 0.95 is defined as mixing ratio. The mixing ratio

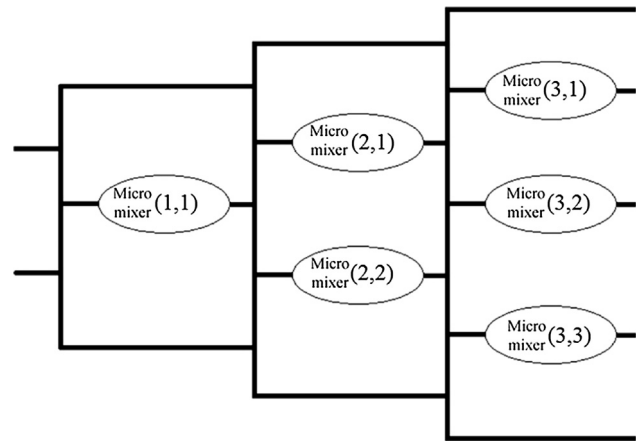

Fig. 8. Schematics of a CGG constructed from a series of micromixers with the same structure and various microchannel depth and fluid flow rate. As the flow rate and dimensions of each micromixer can be varied, finding the mixing length using previous techniques to estimate the mixing length for each micromixer is computationally expensive.

versus channel depths ratio (w/w_0, where w_0 is equal to 0.3 mm) is shown in Fig. 9. It is evident from this figure that using the proposed non-dimensional parameter, ψ, the mixing length in a CGG can be estimated with less than 1% error in the expected mixing fraction.

Similarly, the effect of the flow rate is investigated using various simulations. We conducted another set of 24 simulations in which the flow rate varied from 1.2 to 30 μl/min.

The ratio of the calculated mixing fraction to 0.95 versus the ratio of flow rates (Q/Q_0, where Q_0 is equal to 6 μl/min) is shown in Fig. 10. As the results show, there is no difference in mixing fractions at constant ψ by changing the flow rate of the main microchannel. Therefore, the non-dimensional parameter, ψ, can be used to design a CGG with similar channel structure under different depth as well as flow rate conditions, and this parameter can be used to predict the expected mixing fraction with an error less than 1%.

It is more illuminating to explain these results by considering the diffusion process across the microchannels. If the velocity of the bulk flow increases, little time is available for diffusive mixing. So, the required mixing length will be increased. Conversely, decreasing flow velocity will decrease the mixing length. Keeping the flow rate and width of the microchannel constant, the flow velocity is lower in deeper microchannels. Thus, the fluid in deeper microchannels needs less time to diffuse and reach the side walls. Hence, the mixing length is shorter in deeper microchannels. Conversely, by increasing the fluid diffusivity, diffusion would be more rapid, so smaller mixing length is needed. These linear relations can also be inferred from the governing equation of mass transport (Eq. (4)).

Our simulations confirm that changing the depth of microchannel or the fluid flow rate has no effect on ψ. This can readily be explained according to the definition of ψ, i.e., $\psi = x_{mixing}Dw/LQ$. As discussed before, by increasing the flow rate (Q), the mixing length increases while increasing the width of the channel (w) decreases the mixing length. So, under both conditions, ψ remains constant. Although in our analytical derivation of ψ, we ignored the entrance region and assumed an average stream velocity instead of the parabolic velocity profile, our numerical simulation showed that considering these conditions can only alter the numerical value of ψ. For straight microchannels, we found the value of ψ as 0.28 and 0.22 analytically and numerically, respectively.

It is evident from the above discussion that the defined dimensionless mixing length is not changed by altering the geometric or

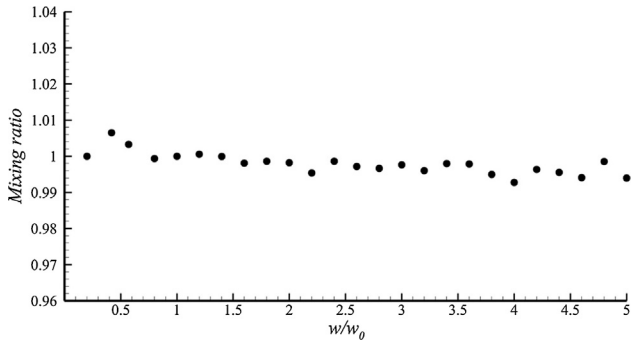

Fig. 9. Mixing ratio versus the channel depths ratio (w/w_0) with $w_0 = 0.3$ mm; mixing ratio is defined as the ratio of mixing fraction in the corresponding mixing length of the channel with a depth of w (constant ψ) to 0.95.

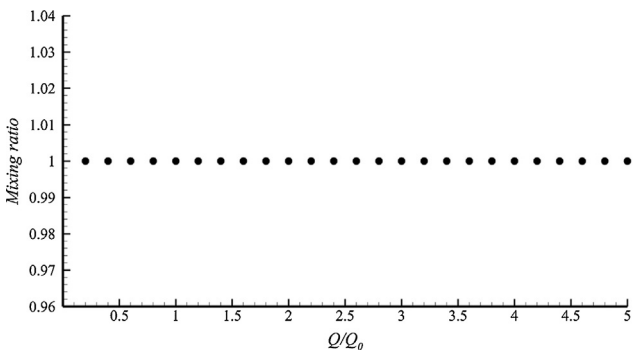

Fig. 10. Mixing ratio versus the flow rates ratio (Q/Q_0) with $Q_0 = 6$ μl/min; mixing ratio is defined as the ratio of mixing fraction in the corresponding mixing length of the channel with a flow rate of Q (constant ψ) to 0.95.

hydrodynamic parameters in an individual type of micromixer. As shown in Fig. 8, different values of mixing lengths of various micromixers placed in several branches of a CGG can be attributed to the differences in the flow rate and channel dimensions. One can compute ψ for a micromixer with desired structure in a CGG for specific dimensions and flow rate condition and then generalize it for all other micromixers with different dimensions and under different hydrodynamic conditions in that CGG structure. As such, introducing a dimensionless mixing length, which is independent of the flow rate and channel dimensions, can substantially facilitate designing a CGG.

4. Conclusion

In this study, a non-dimensional parameter, ψ, was introduced for the mixing process in a micromixer. Using an analytical approach, the value of ψ for a straight micromixer was approximated. Then, we used numerical simulation to find the precise values of ψ in two different micromixers with straight and serpentine configurations. These values (0.22 and 0.17 for straight and serpentine micromixers, respectively) were also validated experimentally. The numerical simulation showed that ψ should be constant for all micromixers with the same structure and is not a function of flow rate or channel sizes (the ratio of channel width to depth).

The main goal of this paper was to define a non-dimensional parameter, ψ, which was constant by changing the flow rate or the cross-sectional area of a micromixer. Using this non-dimensional parameter dramatically facilitates the designing of a CGG. It is sufficient to simulate only one of the micromixers of a CGG and obtain the value of its corresponding ψ. In the next step, knowing that ψ remains constant by changing the flow rate or the channel dimensions, the mixing length of the other micromixers in that CGG can be easily computed. Accordingly, using this non-dimensional mixing parameter is extremely helpful for more effectively designing CGGs.

Conflicts of interest

The authors declare no conflicts of interest.

References

Chiu, D.T., Di Carlo, D., Doyle, P.S., Hansen, C., Maceiczyk, R.M., Wootton, R.C., 2017. Small but perfectly formed? Successes, challenges, and opportunities for microfluidics in the chemical and biological sciences. Chem 2, 201–223.
Chung, B.G., Flanagan, L.A., Rhee, S.W., Schwartz, P.H., Lee, A.P., Monuki, E.S., Jeon, N. L., 2005. Human neural stem cell growth and differentiation in a gradient-generating microfluidic device. Lab Chip 5, 401–406.
Dertinger, S.K., Chiu, D.T., Jeon, N.L., Whitesides, G.M., 2001. Generation of gradients having complex shapes using microfluidic networks. Anal. Chem. 73, 1240–1246.
Duncombe, T.A., Tentori, A.M., Herr, A.E., 2015. Microfluidics: reframing biological enquiry. Nat. Rev. Mol. Cell Biol. 16, 554.
Jeon, N.L., Baskaran, H., Dertinger, S.K., Whitesides, G.M., Van De Water, L., Toner, M., 2002. Neutrophil chemotaxis in linear and complex gradients of interleukin-8 formed in a microfabricated device. Nat. Biotechnol. 20, 826.
Jeon, N.L., Dertinger, S.K., Chiu, D.T., Choi, I.S., Stroock, A.D., Whitesides, G.M., 2000. Generation of solution and surface gradients using microfluidic systems. Langmuir 16, 8311–8316.
Kashaninejad, N., Nikmaneshi, M.R., Moghadas, H., Kiyoumarsi Oskouei, A., Rismanian, M., Barisam, M., Saidi, M.S., Firoozabadi, B., 2016. Organ-tumor-on-a-chip for chemosensitivity assay: a critical review. Micromachines 7, 130.
Kashaninejad, N., Shiddiky, M.J.A., Nguyen, N.-T., 2018. Advances in microfluidics-based assisted reproductive technology: from sperm sorter to reproductive system-on-a-chip. Adv. Biosyst. 2, 1700197. doi:1700110.1701002/adbi.201700197.
Khademhosseini, A., Langer, R., 2016. A decade of progress in tissue engineering. Nat. Protocols 11, 1775.
Lee, C.-Y., Chang, C.-L., Wang, Y.-N., Fu, L.-M., 2011. Microfluidic mixing: a review. Int J Mol Sci 12.
Lin, F., Saadi, W., Rhee, S.W., Wang, S.-J., Mittal, S., Jeon, N.L., 2004. Generation of dynamic temporal and spatial concentration gradients using microfluidic devices. Lab Chip 4, 164–167.
Linshiz, G., Jensen, E., Stawski, N., Bi, C., Elsbree, N., Jiao, H., Kim, J., Mathies, R., Keasling, J.D., Hillson, N.J., 2016. End-to-end automated microfluidic platform for synthetic biology: from design to functional analysis. J. Biol. Eng. 10, 3.
Liu, M., 2011. Computational study of convective–diffusive mixing in a microchannel mixer. Chem. Eng. Sci. 66, 2211–2223.
Moghadas, H., Saidi, M.S., Kashaninejad, N., Nguyen, N.-T., 2017. Challenge in particle delivery to cells in a microfluidic device. Drug Deliv. Trans. Res.
Nguyen, N.-T., Shaegh, S.A.M., Kashaninejad, N., Phan, D.-T., 2013. Design, fabrication and characterization of drug delivery systems based on lab-on-a-chip technology. Adv. Drug Deliv. Rev. 65, 1403–1419.
Nimafar, M., Viktorov, V., Martinelli, M., 2012. Experimental comparative mixing performance of passive micromixers with H-shaped sub-channels. Chem. Eng. Sci. 76, 37–44.
Sackmann, E.K., Fulton, A.L., Beebe, D.J., 2014. The present and future role of microfluidics in biomedical research. Nature 507, 181.
Suh, Y.K., Kang, S., 2010. A review on mixing in microfluidics. Micromachines 1, 82–111.
Toh, A.G., Wang, Z., Yang, C., Nguyen, N.-T., 2014. Engineering microfluidic concentration gradient generators for biological applications. Microfluidics Nanofluidics 16, 1–18.
Walker, G.M., Sai, J., Richmond, A., Stremler, M., Chung, C.Y., Wikswo, J.P., 2005. Effects of flow and diffusion on chemotaxis studies in a microfabricated gradient generator. Lab Chip 5, 611–618.
Wan, J.H., 1965. Self-diffusion coefficients of water. J. Phys. Chem. 69. 4412 4412.
Wang, L., Liu, D., Wang, X., Han, X., 2012. Mixing enhancement of novel passive microfluidic mixers with cylindrical grooves. Chem. Eng. Sci. 81, 157–163.
Wang, S.-J., Saadi, W., Lin, F., Nguyen, C.M.-C., Jeon, N.L., 2004. Differential effects of EGF gradient profiles on MDA-MB-231 breast cancer cell chemotaxis. Exp. Cell Res. 300, 180–189.
Wang, X., Liu, Z., Pang, Y., 2017. Concentration gradient generation methods based on microfluidic systems. RSC Adv. 7, 29966–29984.
Wang, Y., Mukherjee, T., Lin, Q., 2006. Systematic modeling of microfluidic concentration gradient generators. J. Micromech. Microeng. 16, 2128.
Wu, Z., Nguyen, N.-T., 2005. Convective–diffusive transport in parallel lamination micromixers. Microfluidics Nanofluidics 1, 208–217.
Wu, Z., Nguyen, N.-T., Huang, X., 2004. Nonlinear diffusive mixing in microchannels: theory and experiments. J. Micromech. Microeng. 14, 604.
Zilionis, R., Nainys, J., Veres, A., Savova, V., Zemmour, D., Klein, A.M., Mazutis, L., 2017. Single-cell barcoding and sequencing using droplet microfluidics. Nat. Protocols 12, 44.